Available online at www.sciencedirect.com
ScienceDirect
Applied Clay Science 34 (2006) 105–124
Applied CLAY Science
www.elsevier.com/locate/clay

Surface charge heterogeneity of kaolinite in aqueous suspension in comparison with montmorillonite

Etelka Tombácz *, Márta Szekeres

University of Szeged, Department of Colloid Chemistry, H-6720 Szeged, Aradi Vt. 1, Hungary

Received 16 September 2005; accepted 25 May 2006
Available online 1 September 2006

Abstract

An analogous study to 2:1 type montmorillonite [Tombácz, E., Szekeres, M., 2004. Colloidal behavior of aqueous montmorillonite suspensions: the specific role of pH in the presence of indifferent electrolytes. Appl. Clay Sci. 27, 75–94.] was performed on 1:1 type kaolinite obtained from Zettlitz kaolin. Clay minerals are built up from silica tetrahedral (T) and alumina octahedral (O) layers. These lamellar particles have patch-wise surface heterogeneity, since different sites are localized on definite parts of particle surface. pH-dependent charges develop on the surface hydroxyls mainly at edges besides the permanent negative charges on silica basal plane due to isomorphic substitutions. Electric double layers (edl) with either constant charge density on T faces (silica basal planes) or constant potential at constant pH on edges and O faces (hydroxyl-terminated planes) form on patches. The local electrostatic field is determined by the crystal structure of clay particles, and influenced by the pH and dissolved electrolytes. The acid–base titration of Na-kaolinite suspensions showed analogous feature to montmorillonite. The initial pH of suspensions and the net proton surface excess vs. pH functions shifted to the lower pH with increasing ionic strength indicating the presence of permanent charges in both cases, but these shifts were smaller for kaolinite in accordance with its much lower layer charge density. The pH-dependent charge formation was similar, positive charges in the protonation reaction of (Si–O)Al–OH sites formed only at pHs below ~6–6.5, considered as point of zero net proton charge (PZNPC) of kaolinite particles. So, oppositely charged surface parts on both clay particles are only below this pH, therefore patch-wise charge heterogeneity exists under acidic conditions. Electrophoretic mobility measurements, however, showed negative values for both clays over the whole range of pH showing the dominance of permanent charges, and only certain decrease in absolute values, much larger for kaolinite was observed with decreasing pH below pH ~ 6. The charge heterogeneity was supported by the pH-dependent properties of dilute and dense clay suspensions with different NaCl concentrations. Huge aggregates were able to form only below pH ~ 7 in kaolinite suspensions. Coagulation kinetics measurements at different pHs provided undisputable proofs for heterocoagulation of kaolinite particles. Similarly to montmorillonite, heterocoagulation at pH ~ 4 occurs only above a threshold electrolyte concentration, which was much smaller, only ~1 mmol l^{-1} NaCl for kaolinite, than that for montmorillonite due to the substantial difference in particle geometry. The electrolyte tolerance of both clay suspensions increased with increasing pH, pH ~6–6.5 range was sensitive, and even a sudden change occurred above pH ~ 6 in kaolinite. There was practically no difference in the critical coagulation concentration of kaolinite and montmorillonite (c.c.c.~100 mmol l^{-1} NaCl) measured in alkaline region, where homocoagulation of negatively charged lamellae takes place. Rheological measurements showed shear thinning flow character and small thixotropy of suspensions at and above pH ~ 6.7 proving the existence of repulsive interaction between uniformly charged particles in 0.01 M NaCl for both

* Corresponding author. Tel.: +36 62 544212; fax: +36 62 544042.
E-mail address: tombacz@chem.u-szeged.hu (E. Tombácz).

doi:10.1016/j.clay.2006.05.009

clays. The appearance of antithixotropy, the sudden increase in yield values, and also the formation of viscoelastic systems only at and below pH ~ 6 verify the network formation due to attraction between oppositely charged parts of kaolinite particles. Under similar conditions the montmorillonite gels were thixotropic with significant elastic response.

Keywords: Kaolinite; pH-dependent charges; Aggregation; Coagulation kinetics; Dynamic light scattering; Rheology

1. Introduction

Clays are finely divided crystalline aluminosilicates. The principal building elements of the clay minerals are two-dimensional arrays of silicon–oxygen tetrahedra (tetrahedral silica sheet) and that of aluminum- or magnesium-oxygen-hydroxyl octahedra (octahedral, alumina or magnesia sheet). Sharing of oxygen atoms between silica and alumina sheets results in two- or three-layer minerals, such as 1:1 type kaolinite built up from one silica and one alumina sheet (TO), or 2:1 type montmorillonite, in which an octahedral sheet shares oxygen atoms with two silica sheets (TOT) (Van Olphen, 1963; Schulze, 2002). Clay lamellae have negative charge sites on the basal planes owning to the substitution of the central Si- and Al-ions in the crystal lattice for lower positive valence ions. The degree of isomorphic substitution is different, therefore the layer charge density of clay minerals shows high variety. This excess of negative lattice charge is compensated by the exchangeable cations. Additional polar sites, mainly octahedral Al–OH and tetrahedral Si–OH groups, are situated at the broken edges and exposed hydroxyl-terminated planes of clay lamellae (Johnston and Tombácz, 2002). The amphoteric sites are conditionally charged, and so either positive or negative charges, depending on the pH, can develop on the O faces and at the edges by direct H^+/OH^- transfer from aqueous phase. This surface charge heterogeneity of clay minerals presented originally by Van Olphen (1963), then supported and elaborated further in many subsequent and recent investigations (e.g. Zhao et al., 1991; Zhou and Gunter, 1992; Keren and Sparks, 1995; Schroth and Sposito, 1997; Tombácz, 2002; Tombácz, 2003) governs the particle interactions in clay mineral suspensions. Although the overall particle charge is negative in general, both negatively and positively charged parts on the surface of clay mineral particles exist simultaneously under acidic conditions.

The pH-dependent colloidal behavior and the unique surface charge heterogeneity of montmorillonite platelets were the subject of our recent paper in Applied Clay Science (Tombácz and Szekeres, 2004). The simultaneous effect of pH and indifferent electrolytes on the colloidal behavior of montmorillonite suspensions was analyzed. The development of patch-wise surface charge heterogeneity on montmorillonite particles dispersed in aqueous solutions due to crystal lattice imperfections and surface protolytic reactions of edge OH groups was explained. The local electrostatic field formed around the highly asymmetric montmorillonite platelets (in respect of both the aspect ratio and surface charging of edges and faces) was modeled introducing the dominant electric double layer (edl) with constant charge density (σ_0) on the face of lamella and the hidden edl with constant potential at constant pH ($\psi_{0,H}$) at the edges, which are formed and neutralized by the clouds of counter ions (charge densities of diffuse layers, $\sigma_{d,f}$ and $\sigma_{d,e}$, for faces and edges, respectively). As stated the pH of aqueous medium has two kinds of specific role, one is the high affinity of H^+ ions to neutralize the permanent negative charges of dominant electric double layer on faces, and the other is providing chemical species (H^+ and OH^-) to the surface protolytic reactions on edge sites, in which the pH-dependent hidden electric double layer forms. Besides the specific role of pH, the effect of indifferent electrolytes on particle charge heterogeneity was also analyzed, since the extreme geometry of montmorillonite lamellae allows that dominant edl extending from the particle faces spills over at low salt concentration, when the thickness of edl (Debye length, e.g. ~ 3 nm at 10 mM) is larger than that of the thin lamella (~ 1 nm). Therefore the hidden edl at the edge region can emerge only above a threshold of electrolyte concentration estimated between 10 and 100 mM. We could state that the surface charge heterogeneity is not a general feature of montmorillonite particles, it exists only in aqueous medium at pHs below the point of zero charge (PZC) of edge site (~ 6.5) and becomes perceptible above a threshold of electrolyte concentration (20–30 mM NaCl), when the dominant edl remains localized on basal plane.

An analogous study on kaolinite was performed. The objective of present work is to show the essential differences originating from the crystal structure (TOT and TO) in the geometry and the layer charge density between montmorillonite and kaolinite, and to explain the simultaneous effect of pH and indifferent electrolyte on

the formation and neutralization of surface charges on kaolinite particles dispersed in aqueous solutions using dilute and concentrated suspensions under controlled pH and ionic strength conditions.

The differences in surface charge heterogeneity between different clay particles manifested remarkably in a recent paper (Wan and Tokunaga, 2002). The partitioning of clay colloids at air–water interface was studied. Reference samples of Clay Mineral Society was used to test particle accumulation. Kaolinite (KGa1), illite (IMt-2) and montmorillonite (SWy-2) were measured in NaCl solutions under varying pH and ionic strength conditions. Montmorillonite lamellae were excluded from the air–water interface at any pH in 0.001 M NaCl and up to 0.1 M at pH ~ 5.5, while kaolinite particles exhibited extremely high affinity to the negatively charged air–water interface below pH ~ 7, if NaCl concentration was at least 0.001 M. These clay particles were definitely different in respect of geometry and surface charge properties. It is worth recalling the data of Wan and Tokunaga (2002) relevant to the subject of present paper (Table 1). The aspect ratio (diameter/thickness) 2 to 10 was measured for kaolinite particles, which is extremely different from that of montmorillonite lamellae estimated as ~500 or even larger. Much pronounced role of edge area in surface charge properties can be predicted for kaolinite as for montmorillonite, especially, if the difference in the structural charge densities being responsible for permanent charges is also taken into consideration.

High-resolution transmission electron microscopy (HRTEM) examinations (Ma and Eggleton, 1999b) have indicated that three types of surface layers may exist in natural kaolinite crystals. Type 1 has the expected 0.7 nm TO surface layer as terminations. Type 2 has one 1 nm pyrophyllite-like (TOT) layer as the surface layer on one side of a kaolinite particle, the spacing between the TOT and the adjacent TO layer is not expandable. Type 3 kaolinite has one or several TOT collapsed smectite-like layers at one or both sides of a stack forming a special kind of kaolinite–smectite interstratification, which has only been recognized in some poorly-ordered kaolinites. The surface smectite layer(s) contribute to higher cation exchange capacity (CEC) values. The same authors (Ma and Eggleton, 1999a) determined the CEC of several kaolinite samples and compared them to theoretical calculations of CEC. This comparison revealed that the exchangeable cations occur mostly on the edges and on the basal (OH) surfaces of kaolinite. It was also shown that permanent negative charge from isomorphic substitution of Al^{3+} for Si^{4+} is insignificant, and that the CEC of kaolinite strongly depends on the particle size (both thickness and diameter in the 00l plane) and the pH value. This study revealed that the hydroxyls on the exposed basal surfaces may be ionizable in aqueous solutions, and the amount of negative charge on the edges and the exposed basal hydroxyls depends on pH and other ion concentrations.

Table 1
Size, shape, and charge properties of kaolinite KGa-1 and montmorillonite SWy-2 (data from Wan and Tokunaga, 2002)

Clay mineral	Size nm	Structural charge sites/nm^2	Estimated thickness nm	Edge area % of total
Kaolinite	<~500	~0.3	40 to 70	20 to 30
Montmorillonite	>~500	~14.9	1	<1

The development of pH-dependent surface charges on kaolinite was explained by proton donor–acceptor reactions taking place simultaneously on basal planes and edges (Brady et al., 1996). Based on the measured proton adsorption isotherms and molecular modeling of proton-relaxed kaolinite structure, authors proved the substantial contribution of edge Al sites to the pH-dependent charge development due to thicker particles.

The acid–base chemistry of clay minerals with permanent and variable charges was described by using surface complexation model, and its applications to montmorillonite and kaolinite were presented (Kraepiel et al., 1998). Protonation–deprotonation reactions were supposed to take place both on the edges (≡Al–OH groups) and on the gibbsite basal planes (Al–O–Al groups). Authors noted that kaolinite does not correspond exactly to the model solid, the distribution of permanent and variable charges is not uniform on the surface of particles.

Although the substantial difference in the pH-dependent behavior of clay minerals is known from sixties (Van Olphen, 1963), a unified triple layer model of clay minerals was still proposed and applied for smectite (2:1 type) and kaolinite (1:1 type) recently (Leroy and Revil, 2004). Authors emphasized that both chemical and electrical characters of clay particles were considered referring to the similar work of Avena and De Pauli (1998) published previously, meanwhile the significant differences in geometry and electric double layers of clay particles with patch-wise charge heterogeneity were ignored. Probably this also contributed to the chemical nonsense in surface site speciation calculated for kaolinite edges (Leroy and Revil, 2004). It has to be mentioned, only the montmorillonite was investigated in the referred paper (Avena and De Pauli, 1998), and authors assumed the presence of smear-out charges and potentials for 2:1 type clay particles in their surface speciation model as an acceptable approximation. The proton binding at clay–water interfaces for both 2:1 and

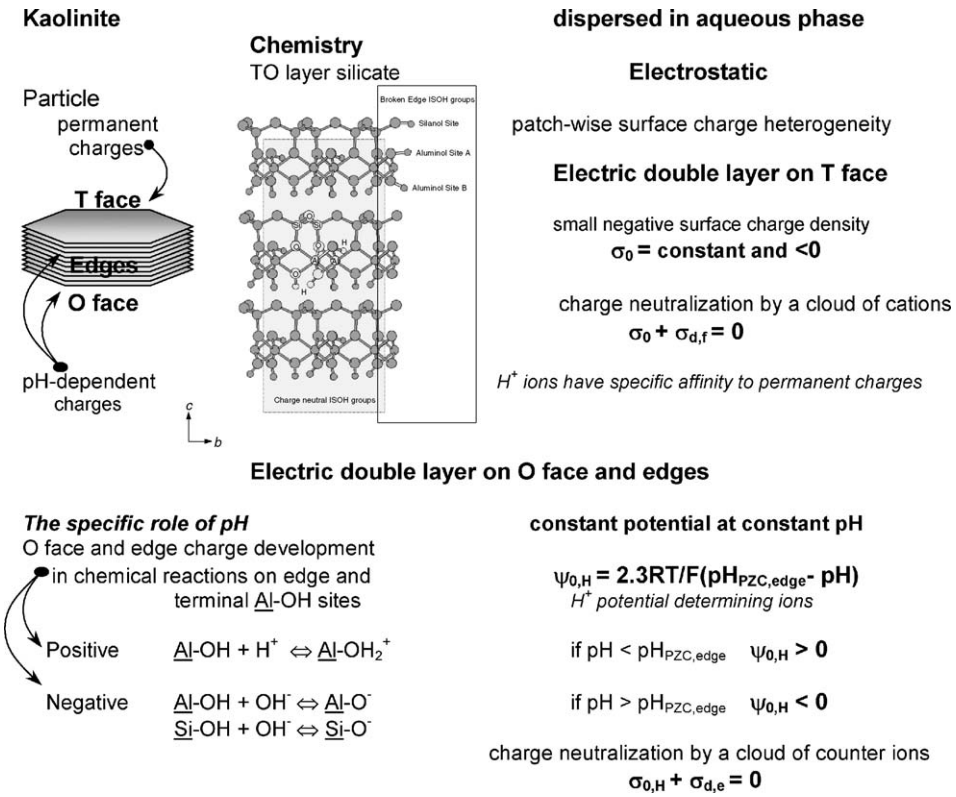

Fig. 1. Development of patch-wise surface charge heterogeneity on 1:1 type kaolinite (atom arrangement in silica tetrahedral (T) and alumina octahedral (O) layers inserted) particles dispersed in aqueous solutions due to crystal lattice imperfections (permanent negative charges on T faces) and surface protolytic reactions of edge and O face OH groups (pH-dependent charges on edges). An electric double layer (edl) with constant charge density (σ_0) on the T face of particle, while another edl with constant potential at constant pH ($\psi_{0,H}$) on its edges and O face are formed, and both are neutralized by the clouds of counter ions (charge densities of diffuse layers, $\sigma_{d,f}$ and $\sigma_{d,e}$, for T face and edges, respectively).

1:1 type clay particles is discussed in one of their recent work (Avena et al., 2003). The proton affinity of different surface sites located on basal plane and at broken edges was analyzed on the basis of MUSIC model. They concluded that siloxane and gibbsite-like groups on the basal surface of 2:1 and 1:1 clays are not reactive, however, the protonation–deprotanation reactions take place on the Al–OH sites, while Si–OH sites are unreactive at the broken edges under normal pH conditions. Additionally, the reactivity of edge groups is also influenced by the presence of structural charges, and the electric field originating from the permanent charges affects on both the basal and the edge surface reactions.

The pH-dependent electro-osmotic flows observed in NaCl-water saturated kaolinite system were modeled successfully in a recent paper (Dangla et al., 2004) using similar approach to ours introduced for montmorillonite (Tombácz and Szekeres, 2004; Tombácz et al., 2004). In the case of kaolinite the low level of isomorphic substitution (1–8 meq/100 g), i.e. the low permanent charge density (−0.064 to −0.5 C/m^2) and the significance of Al–OH sites in the formation of pH-dependent charges were underlined. We should note that this range of charge density is not low at all, especially comparing it with the permanent charge density of montmorillonite up to about −0.1 C/m^2 (Van Olphen, 1963; Tombácz et al., 1990; Kraepiel et al., 1998).

As explained for montmorillonite before (Tombácz and Szekeres, 2004) and supported for clay colloids (Wan and Tokunaga, 2002), the effect of pH and indifferent electrolytes is mutual; none of them can be interpreted alone. Now we attempt to outline schematically how the material characteristics of kaolinite govern the formation of local electrostatic field around the relatively robust, less asymmetric clay particle than montmorillonite lamella in respect of both the aspect ratio and surface charge density in aqueous medium containing indifferent electrolytes besides the autoprotolytic products of water in Figs. 1 and 2.

Unlike the 2:1 montmorillonite having two planar siloxane surfaces per TOT layer, the 1:1 layers of kaolinite (crystal structure showed in Fig. 1) are bound together in the c direction by hydrogen bonds between hydroxyl groups of octahedral (O) sheet and the highly electronegative oxygens of the silicon tetrahedral (T) sheet. Therefore a kaolinite particle has one siloxane and one hydroxyl surface, T and O faces, respectively. This corresponds to the Type 1 surface layer as terminations (Ma and Eggleton, 1999b). Minor isomorphic substitution in the tetrahedral sheet results in a few permanent negative charges on the T face. This excess of negative lattice charge is compensated by the exchangeable cations in the diffuse part of the electric double layer (edl) on T faces (Fig. 2). Two types of inorganic surface hydroxyl groups (ISOH) occur in the solid phase of different minerals (Johnston and Tombácz, 2002) as illustrated for kaolinite in Fig. 1. The first type is charge neutral ISOH groups, which are the part of the crystal structure. They are coordinated to metal atoms whose coordination environment is complete. The second ISOH, silanol and aluminol groups that occur on broken edges and gibbsite planes, are bound to undercoordinated metal atoms, they are more reactive. The O face hydroxyl groups are probably less reactive than edge aluminols and silanols (Brady et al., 1996; Avena et al., 2003), but not all papers distinguish between them (Coppin et al., 2002; Dangla et al., 2004). The pH-dependent charges, either positive or negative as shown in Fig. 1, can develop on these amphoteric sites at the edges and O faces by direct H^+ or OH^- transfer from aqueous phase. The variable edge charges are compensated by a cloud of counter ions in the electric double layers at edges and O faces presented schematically at different electrolyte concentrations in Fig. 2. The patchwise charge heterogeneity can develop on the different parts of kaolinite particle, if the pH of aqueous solution is lower than the point of zero charge (PZC) of amphoteric (mainly edge) sites, which is about 3 to 4 (Appel et al., 2003), 3.8 (Brady et al., 1996), 5.5 (Dangla et al., 2004), 4–5.5 (Coppin et al., 2002), 5.9 (Kretzschmar et al., 1998) or ranging from pH 5 to 9 depending on the kaolinite used, the clay pretreatment, and the method used for its determination as stated in the paper of Kretzschmar et al. (1998). However, at very low electrolyte concentration ($<\sim 0.001$ M), where the thickness of edl (Debye length, e.g. ~ 10 nm at 0.001 M) is comparable with the thickness of kaolinite particle (10–120 nm (Brady et al., 1996), 40–70 nm (Wan and Tokunaga, 2002)), the oppositely charged parts cannot see each other (top of Fig. 2). These emerged at higher, only above a heterocoagulation threshold of electrolyte concentration (bottom of Fig. 2) as introduced for the interaction of oppositely charged magnetite and montmorillonite particles before (Tombácz et al., 2001), and the attraction between the oppositely charged parts results in heterocoagulated aggregates. The edge(+)/face(−) interactions in kaolinite suspensions are more important than that for montmorillonite, because the particles are thicker (Penner and Lagaly, 2001).

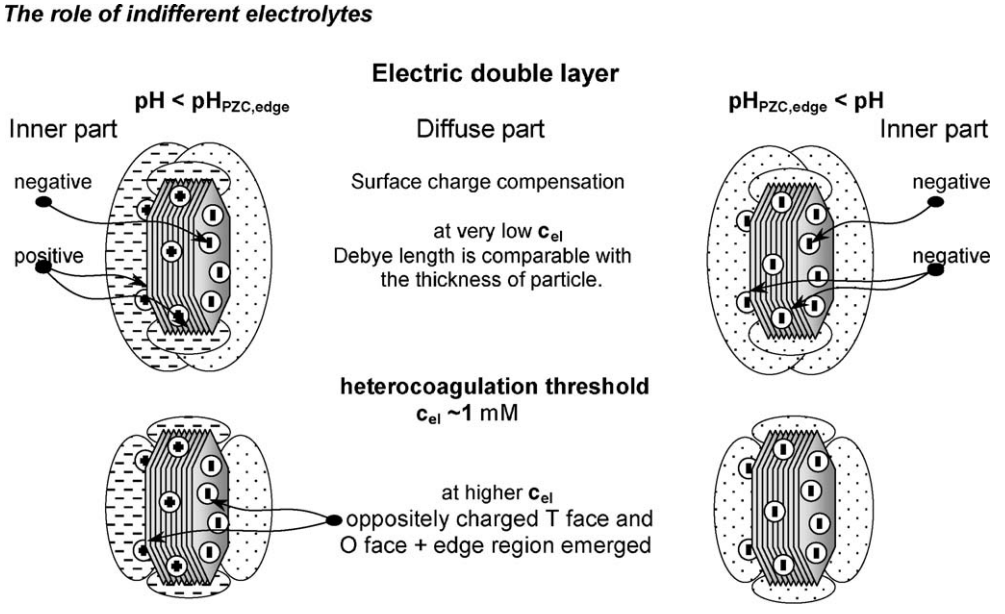

Fig. 2. Schematic representation of the electric double layers forming around the kaolinite particles under different solution conditions. The effect of indifferent electrolytes on particle charge heterogeneity besides the specific role of pH.

2. Experimental

2.1. Preparation of kaolinite suspensions

Kaolinite was obtained from Zettlitz kaolin (Germany). An aqueous slurry of kaolin was treated with Na_2CO_3 at about 80 °C for 2 days then diluted by Millipore water up to 4 g clay in 100 ml suspension. Kaolinite fraction smaller than 2 μm was prepared by allowing the larger particles to settle down in the clay suspensions and then decanting. The excess carbonate was eliminated by HCl addition. To obtain the monocationic Na-kaolinite, the suspension was treated with 1 M NaCl. After centrifugation of the suspensions at 3600 RPM, the supernatant solution was discarded and replaced with fresh solution. The procedure was repeated three times. The ionic strength of suspension was progressively lowered, first by washing with Millipore water and then by dialysis against 0.01 M NaCl, to that used in the experiments. The progress of dialysis was controlled by measuring conductivities of inner and outer phases daily. Na-kaolinite suspension (~200 g/l) in dialysis tubes reached equilibrium state within 2 weeks. This procedure provides a definite initial state with constant ionic strength at self-pH of suspensions for further work. The stock suspensions were stored in refrigerator at 4–5 °C. The smaller electrolyte concentration of medium was reached by dilution. Freeze-dried sample was prepared to measure cation exchange capacity (CEC) and specific surface area. CEC value was 9 meq/100 g. Specific surface area determined by nitrogen adsorption (BET) was 83 m^2/g. X-ray diffraction pattern of air-dried and ethylene glycol saturated kaolinite samples on glass plates was determined to check the presence of smectite impurity. Measurement was performed over the scanning range $2° < 2\Theta < 40°$ at room temperature by using a Philips PW 1830 X-ray generator with CuK_α ($\lambda = 0.154$ nm) radiation and a Philips PW 1820 goniometer operating in the reflection mode. The characteristic reflections (d_{001} 0.72 nm and d_{002} 0.36 nm) of kaolinite (Van Olphen and Fripiat, 1979) in both states can be shown in Fig. 3. For the sake of comparison the XRD pattern of Na-montmorillonite taken before (Tombácz and Szekeres, 2004) is also shown. The presence of swelling clays in kaolinite cannot be revealed, since no any reflection at ~7° 2Θ appeared in the kaolinite sample swelled in ethylene glycol. It should be noted that the surface smectite layer(s) contribute to higher CEC values cannot be detected by XRD (Ma and Eggleton, 1999b). The water was obtained directly from a Millipore apparatus. All the used chemicals were analytical reagent grade product (Reanal, Hungary).

2.2. Potentiometric acid–base titration

The pH-dependent surface charge was determined by potentiometric acid–base titration under a CO_2-free atmosphere using electrolyte NaCl to maintain a constant ionic strength 0.01, 0.1 and 1 M, respectively. Before titration the suspensions containing ~1 g kaolinite were stirred and bubbled with purified nitrogen for an hour. Equilibrium titration was performed by means of a self-developed titration system (GIMET1) with 665 Dosimat (Metrohm) burettes, nitrogen bubbling, magnetic stirrer, and high performance potentiometer at 25±1 °C. The whole system (mV-measure, stirring, bubbling, amount and frequency of titrant) was controlled by IBM PS/1 computer using AUTOTITR software. A Radelkis OP-0808P (Hungary) combination pH electrode was calibrated for three buffer solutions to check the Nernstian response. The hydrogen ion activity vs. concentration relationship was determined from reference electrolyte solution titration, so that the electrode output could be converted directly to hydrogen ion concentration instead of activity. In the first cycle, suspensions were titrated with standard HCl solution down to pH 3.5 then with standard base solution (NaOH) up to pH 9.5, then again with acid solution in the third cycle. The titration was not reversible within the reproducibility of this method, the curves measured in the direction of decreasing and increasing pH (backward and forward curves, respectively) showed small hysteresis at each ionic strength, although the acid–base titrations were performed in the range of pH probably free of dissolution ($[Al^{3+}] \sim 10^{-3.5}$ M at pH ~ 3.5 and $[Al(OH)_4^-] \sim 10^{-5}$ M at pH ~ 9.5 in Bolt and Bruggenwert (1978); the dissolved Al concentration in the equilibrium aqueous phase of

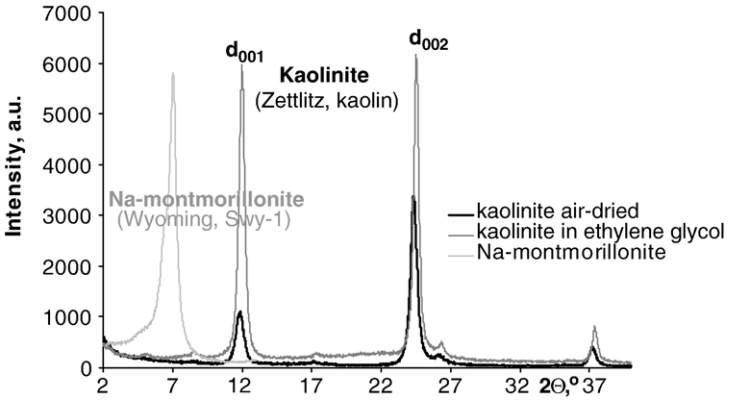

Fig. 3. XRD patterns of air-dried and ethylene glycol saturated kaolinite samples on glass plates in comparison with that of Na-montmorillonite (Wyoming, Swy-1 sample).

kaolinite suspensions after 3 days remained below 10^{-4} M over the range of pH from 3 to 9 in Coppin et al., 2002).

The net proton surface excess amount ($\Delta n^{\sigma}_{H/OH}$, mol/g) is defined as a difference of H^+ and OH^- surface excess amounts (n^{σ}_{H+} and n^{σ}_{OH-}, respectively) related to unit mass of solid, $\Delta n^{\sigma}_{H/OH}=n^{\sigma}_{H+}-n^{\sigma}_{OH-}$. The surface excess amount of any solute, like H^+ and OH^- here, can be determined directly from the initial and equilibrium concentration of solute for adsorption from dilute solution (Everett, 1986). The values n^{σ}_{H+} and n^{σ}_{OH-} were calculated at each point of titration from the electrode output using the actual activity coefficient from the slope of H^+/OH^- activity vs. concentration straight lines for background electrolyte titration.

2.3. Electrophoretic mobility measurement

Electrophoretic mobility of kaolinite, montmorillonite and aluminum oxide particles was measured at 25+0.1 °C in a capillary cell (ZET 5104) with ZetaSizer 4 (MALVERN, U.K.) apparatus. Stock dispersions were diluted to ~0.05 g/l solid content and the salt concentration of dilute systems was adjusted to a constant concentration of NaCl (0.01 M). The pH of dilute dispersions were adjusted between ~3 and ~10 by adding either HCl or NaOH solutions, and measured directly before introducing sample in to the capillary cell.

2.4. Dynamic light scattering measurements

Dynamic light scattering (DLS) measurements were performed using a ZetaSizer 4 (MALVERN, U.K.) apparatus operating at λ=633 nm produced by an He–Ne laser at scattering angle 90° at 25±0.1 °C to determine average particle size in dilute suspensions. The stock suspension of kaolinite was diluted ten times by Millipore water (suspension concentration ~20 g/l, ionic strength 0.001 M), and centrifuged at 6000 RPM for half an hour to obtain the fine (<~0.5 μm) kaolinite particles in the supernatant. The fine fraction was diluted by Millipore water solution to reach a constant solid content (~0.1 g/l). Coagulation kinetics measurements were performed at pH ~4, ~6 and ~8 with the series of kaolinite suspensions containing different (from 0.0001 to 0.2 M) final concentrations of NaCl. The desired pH values in the suspensions and in the double concentrated NaCl solutions were preadjusted by HCl and NaOH solutions, respectively, and they were stored in a thermostat at 25±0.1 °C. 1 ml of suspension was placed in the measuring cell and 1 ml of electrolyte solution with the same pH was mixed with it, then size measurement was started after 5 s and continued till 270 s (data collection time: 10 s, time between each sizing: 20 s). Size evolution of aggregates was followed in time. The pH-dependent aggregation of montmorillonite and kaolinite particles was compared at constant ionic strength (0.01 M NaCl). The pH of dilute systems were adjusted in the range from 4 to 10, and measured directly before a sample was placed in the quartz cell. The size measurement was started after 5 min. The correlation functions were evaluated by cumulant analysis (Brown, 1993). Supposing a monomodal distribution a third-order cumulant fitting was used, and the Z-average hydrodynamic size was calculated.

2.5. Rheological measurements

The rheological measurements were performed with a rheometer HAAKE RS 150 and a cone-plate sensor (DC60/2° Ti) at temperature 25±0.1 °C controlled by a HAAKE DC 30/K20 thermostat. Two types of measurements were performed:

- The flow curve (upward) was measured with a shear rate ramp over 1 min from 0 to 100 1/s, then the ramp was reversed to measure downward flow curve. The area between the upward and downward curve was calculated as measure for thixotropy using data analysis option of RheoWin software.
- The creep test was performed to determine the viscoelastic behavior under static condition. A constant stress between 0.01 and 10 Pa was applied for 1 min and the resulting strain was measured (creep), then stress was released and strain was measured for 1 min (recovery). The shear creep compliance (J, 1/Pa) was calculated dividing the measured shear strain (γ) values by the applied stress (τ, Pa).

The dynamic test of viscoelasticity was also attempted in forced oscillation measurements in the range of frequency from 0.01 to 10 Hz, then of stress from 0 to 40 Pa.

15 g/100 g kaolinite suspensions containing 0.01 M NaCl were measured at different pHs from ~5 to ~8. The pHs of dense suspensions were adjusted with adding estimated amounts of 1 M NaOH or HCl solutions. The pHs of well-homogenized suspensions were measured, then all were stored in sealed vials under nitrogen for a day. The portions of suspensions were carefully placed on the measuring plate of rheometer, and the measuring position was reached at low speed. The equilibrium pH values of suspensions were measured after rheological measurements. The pH shift during 1-day-standing was less than 0.2 pH unit.

3. Results and discussion

3.1. Simultaneous pH-dependent charge development on edge and basal OH sites, and H^+/Na^+ ion exchange on permanent negative charge sites

Potentiometric acid–base titration over the range of pH between 3.5 and 9.5 was used to characterize the pH-dependent charge development on the amphoteric surface sites of kaolinite. Protolytic reactions at edges and probably on basal OH faces take place in parallel with the H^+/Na^+ ion exchange on permanent negative charge sites of T faces, and the separation of the individual contribution to the measurable H^+ and OH^- consumption is not possible experimentally. A prudent preparation of kaolinite suspension provided a well-defined initial state

of titration and allowed us to use an evaluation method developed before for oxides (Tombácz and Szekeres, 2001), which assumes only the mass conservation law for H^+/OH^- ions during titration. A constant NaCl concentration in liquid phase and a sufficient Na-saturation of ion exchange sites on faces was reached in an equilibrium dialysis of kaolinite suspension against 0.01 M NaCl. The acid–base titration cycles measured at 0.1 M NaCl concentration are shown in Fig. 4. The net proton consumption curves for Na-kaolinite show a small hysteresis, the backward and forward titration curves in the direction of decreasing and increasing pH, respectively, do not coincide, which is different from that observed in the case of montmorillonite samples (Tombácz and Szekeres, 2004). The net proton consumption curves determined at different salt concentrations showed similar character as seen in Fig. 5. While the acid–base processes in montmorillonite suspensions over the pH range free of dissolution were considered as reversible equilibrium apart from the first downward curves, the analogous titration of kaolinite suspensions did not result in reversible cycles satisfactorily within the experimental error of this method. Therefore the evaluation of kaolinite data would not be correct, if we use the same equilibrium model, which was applied to calculate the pH-dependent charging of montmorillonite (Tombácz et al., 2004).

Similarly to montmorillonite, a decrease in the initial pH of suspensions with increasing salt concentration was observed in kaolinite suspensions, too. However, the extent of pH shift ($\Delta pH = pH_{i,0.01} - pH_{i,1}$) being almost the same ($\Delta pH \sim 0.8$) for the montmorillonite samples, was much smaller ($\Delta pH = 0.44$) in kaolinite suspensions (the initial pH values given in Fig. 4). Since this pH shift is indicative of the permanent negative charges on solid in question according to the basic principles of acid–base surface chemistry of soils (Sposito, 1984), it can be stated that permanent charges are present in kaolinite particles, and the edl developed probably on T faces influences the ion distribution of electrolytes, but the effect of layer charges is much less dominant, than that in montmorillonite suspensions.

The 2:1 layer-type montmorillonite has high permanent layer charge and negligible variable charge (Sposito, 1984; Tombácz et al., 1990; Keren and Sparks, 1995; Mohan and Fogler, 1997; Tombácz et al., 1999), while kaolinite has much lower apparent values, and its amphoteric character is obvious. Comparing the net proton surface excess vs. pH functions of montmorillonite and kaolinite at three different ionic strengths (Fig. 6), which never intersect in contrast with oxides (James and Parks, 1982), it can be seen that their overall H^+/OH^- consumption is similar, although the difference between montmorillonite and kaolinite, besides their crystal structure and layer charge, in specific surface area is about one order of magnitude. Both sets of curves shifted in the direction of lower pH with increasing NaCl concentration, which also indicates the presence of permanent charges. The extent of parallel shift, however, is smaller for the 1:1 type kaolinite than that for 2:1 type montmorillonite in accordance with the about one order of magnitude difference in cation exchange capacity (CEC) value of these samples (9 and 105 meq/100 g for Zettlitz kaolin and Swy-2 montmorillonite, respectively (Tombácz, 2003; Tombácz and Szekeres, 2004)). This significant difference also supports

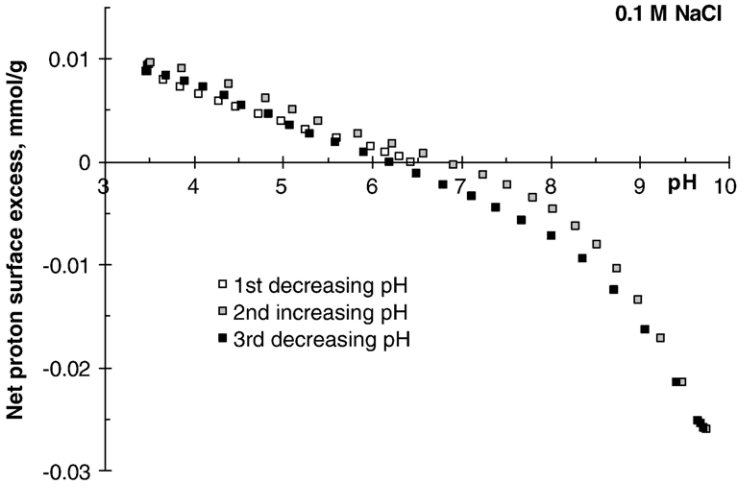

Fig. 4. Experimental net proton surface excess curves for Na-kaolinite in 0.1 M NaCl solution at room temperature. The points were calculated from the data of equilibrium titration cycles to test the reversibility of acid–base processes: first a backward (open symbols) with 0.1 M HCl solution, then a forward (gray symbols) with 0.1 M NaOH solution, finally a backward titration (black symbols) again.

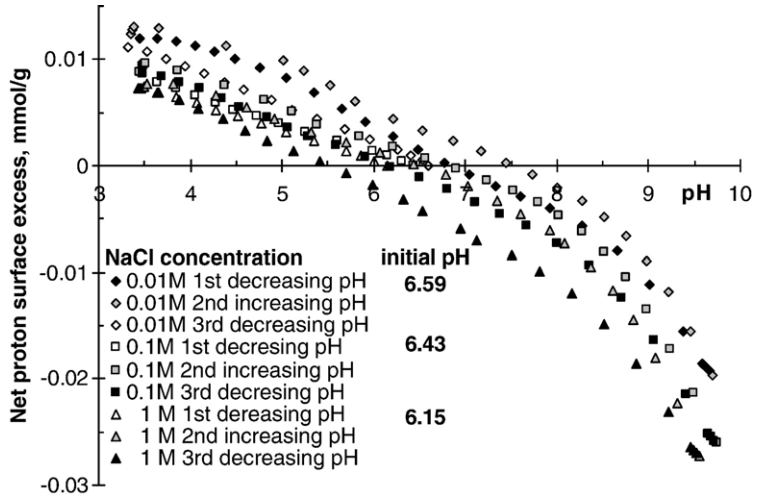

Fig. 5. Experimental net proton surface excess curves for Na-kaolinite dialyzed against 0.01 M NaCl solution, then diluted with NaCl solutions to adjust salt concentrations 0.01, 0.1 and 1 M, respectively, at room temperature. The points were calculated from the data of an equilibrium titration cycles to test the reversibility of acid–base processes: first a backward (open symbols) with 0.1 M HCl, then a forward (gray symbols) with 0.1 M NaOH solution, finally a backward (black symbols) titration again.

our statement above on the influence of layer charge. The much less proton excess amounts in the positive region accords well with the low layer charge density of kaolinite (Bolland et al., 1980; Zhou and Gunter, 1992; Schroth and Sposito, 1997), and the comparable values in the negative region show the more pronounced role of amphoteric sites on kaolinite particle in comparison with montmorillonite.

In the course of the acid–base titration of kaolinite the contribution of amphoteric edge and basal OH (O face) sites to develop variable charges is significant. Besides the limited ion-exchange process for H^+ and Na^+ ions on permanent negative charges ($NaX + H^+ \Leftrightarrow HX + Na^+$), the protonation and deprotonation of aluminol groups in the reactions $\underline{Al}–OH + H^+ \Leftrightarrow \underline{Al}–OH_2^+$ and $\underline{Al}–OH \Leftrightarrow \underline{Al}–O^- + H^+$ takes place in the acidic and alkaline regions, respectively. The protonation of silanol groups at edges is not probable above pH ~ 3.5, since silica surfaces are anionic down to pH ~ 3 (Brady et al., 1996). However, the contribution of silanol groups to the base consumption and negative charge formation in a deprotonation reaction ($\underline{Si}–OH \Leftrightarrow \underline{Si}–O^- + H^+$), especially above pH ~ 8 may be dominant.

The contribution of amphoteric sites to the acid–base properties of kaolinite seems to be significant, but their

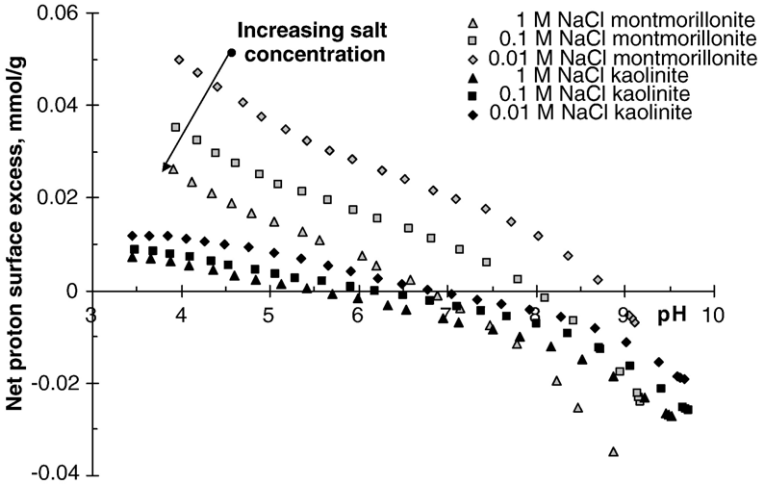

Fig. 6. Comparison of the effect of electrolytes on the pH-dependent surface accumulation of protons determined by acid–base titration for montmorillonite and kaolinite.

effect on charge-potential curves, i.e. opening with increasing electrolyte concentration due to charge screening, which is typical for all amphoteric oxides, does not appear. The pH of zero net proton charge (PZNPC) of kaolinite may be identified at pH ~ 6–6.5. This value is higher than most reported value for specimen kaolinite (Zhou and Gunter, 1992; Schroth and Sposito, 1997), but is close to the published PZNC (point of zero net charge) at pH 7.3–6.6 (Herrington et al., 1992), and the PZC of edge sites at pH 7.5 calculated from the potentiometric titration data corrected with the amount of permanent charges (Blockhaus et al., 1997).

It is worth comparing the results of kaolinite with the ionic strength dependent surface charging of aluminum and silicon oxides in Fig. 7, which are relevant to the edge sites of kaolinite in chemical point of view. Both oxides exhibit the common feature of net proton surface excess vs. pH curves at different ionic strengths. The main difference between the acid–base properties of these oxides is the pHs of their PZC, since it is above pH 8 for alumina and below pH 4 for silica (Tombácz et al., 1995). In the case of kaolinite, however, the reversible net proton surface excess curves at different ionic strengths (Fig. 5) never intersect, no any common intersection point such as PZC or PZSE (point of zero salt effect) can be identified. The extent of proton accumulation on the surface of kaolinite particles is always greater at lower ionic strength similarly to those of the clays in literature (Kraepiel et al., 1998, 1999). Comparing the net proton surface excess vs. pH function measured for kaolinite with that of the alumina and silica samples in Fig. 7, we can conclude that the acid–base properties of amphoteric sites of kaolinite are just between the surface OH bound to the pure Al_2O_3 and SiO_2 solid matrix, similarly to our conclusion based on the SCM modeling for montmorillonite, where we stated that the OH groups at edges having PZC at pH ~ 6.5 as less basic than the Al–OH and less acidic than the Si–OH groups.

Positive charges can develop only on the Al–OH sites of edges and basal OH surfaces at pHs below ~ 6, however, these are not necessarily emerged at very low electrolyte concentration (< ~ 1 mM), when the Debye length is comparable with the thickness of kaolinite particles as shown in Fig. 2. The unique surface charge heterogeneity of kaolinite particles disappears, if the pH of suspensions is above the $pH_{PZC,\ edge}$ ~ 6–6.5, since the deprotonation of Si–OH then that of the Al–OH sites takes place with increasing pH of solution resulting in negative charges at edges and O faces similarly to that on T faces.

3.2. pH-dependent charge state of clay particles in electrolyte solutions

Electrophoretic mobility and zeta potential data hold information on the electric double layer of charged particles. The sign of these measurable electric data is the same as that of the excess charge of particle moving together with the adhered layer of counterions, and its magnitude is somewhat proportional to the particle charge (Hunter, 1981).

The pH-dependent electrophoretic mobility of solid particles holding permanent and/or variable charges is characteristically different as shown for kaolinite,

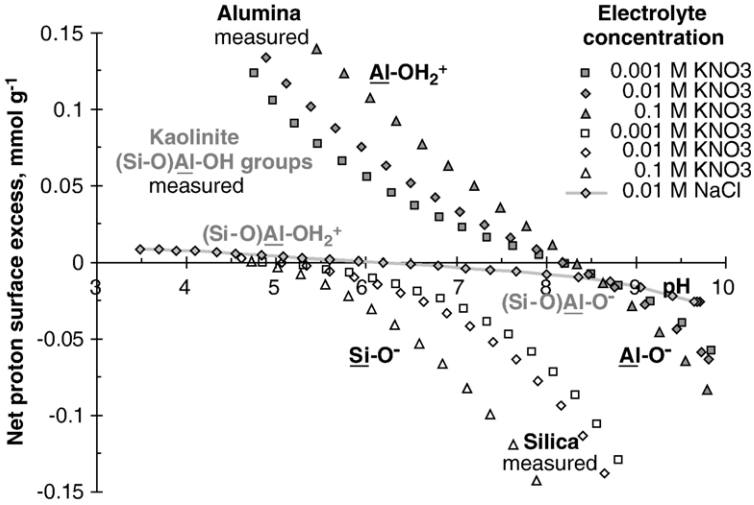

Fig. 7. The pH-dependence of net proton surface excess amounts for different solid materials. Experimental data measured at different ionic strengths for Al_2O_3 (Aluminum Oxide C, Degussa) and SiO_2 (Aerosil 200, Degussa), and for kaolinite at 0.01 M NaCl.

montmorillonite and aluminum oxide particles in Fig. 8. The sign of the mobility measured in the aluminum oxide dispersions reverses at a characteristic pH identified as the pH of isoelectric point (IEP), if this is the intersection point of pH-dependent curves measured at different ionic strengths. The symmetric shape of the mobility–pH plot near the IEP indicates the significance of H^+/OH^- ions in determining surface charging. The pH of sign reversal of electrophoretic mobility (~IEP) in present example is at pH ~ 8 showing clearly that alumina particles are positively charged below and negatively above this characteristic pH, which is close to the pH ~ 8 of PZC determined from the surface charge titration curves of aluminum oxide (Fig. 7). The dominance of permanent negative charges on montmorillonite and even kaolinite particles is obvious from the negative mobility values observed over the whole range of pH. The contribution of positive charges, which develop on the Al–OH sites at exposed hydroxyl-terminated planes of kaolinite and at the edges of both clays at pHs below ~ 7, is not significant as compared to the excess charge of clay particles. A definite bend of the mobility vs. pH curve for kaolinite below pH ~ 6 from that of montmorillonite shows a slight decrease in the net negative particle charge of kaolinite, since the probable amount of protonated Al–OH sites (~ 0.01 mmol/g at pH ~ 4 in Fig. 5), i.e., positive charges below pH ~ 6, becomes comparable with the relative small amount of permanent negative charges on kaolinite surface (CEC ~ 0.09 meq/g). The negative value of electrophoretic mobility and zeta potential measured in montmorillonite suspensions at even acidic pHs in general relates to the dominance of permanent charges, such as here 1.05 meq/g for Swy-2, which is much larger than the amount of edge Al–OH sites 0.03–0.04 mmol/g estimated in our previous model calculation (Tombácz et al., 2004). However, in the case of kaolinite small, but positive values below the pH of isoelectric point (IEP) are often published, such as zeta potential below pH ~ 4.3 (Hu et al., 2003), electrophoretic mobility at pH < 4.8 (Kretzschmar et al., 1998), electroacoustic mobility below pH 3.8–4.1, meanwhile large negative zeta potential values (−26, −28 mV) are also given at pH ~ 4.4 for kaolinite in this paper (Appel et al., 2003) similarly to that of −15 mV at pH ~ 4 (Akbour et al., 2002). This high variety in the overall particle charge in acidic suspensions also supports that the negative layer charge of kaolinite is comparable with the pH-dependent variable charges developing positive charges on edge and O face sites as depicted in Fig. 1 in general, and so the appearance of charge reversal and IEP definitely depends on the kaolinite used, the clay pretreatment, and probably the method used to determine these data.

3.3. Edge-to-face and face-to-face aggregation in dilute suspensions

3.3.1. pH-dependent aggregation of clay particles

The pure clay particles in aqueous medium are electrostatically stabilized from colloidal stability point of view. Particles either aggregate or disperse depending on the structure of electric double layer formed on the particle surface as depicted for kaolinite in Fig. 2 and for montmorillonite before (Tombácz and Szekeres, 2004). Aggregation processes in dilute suspensions can be

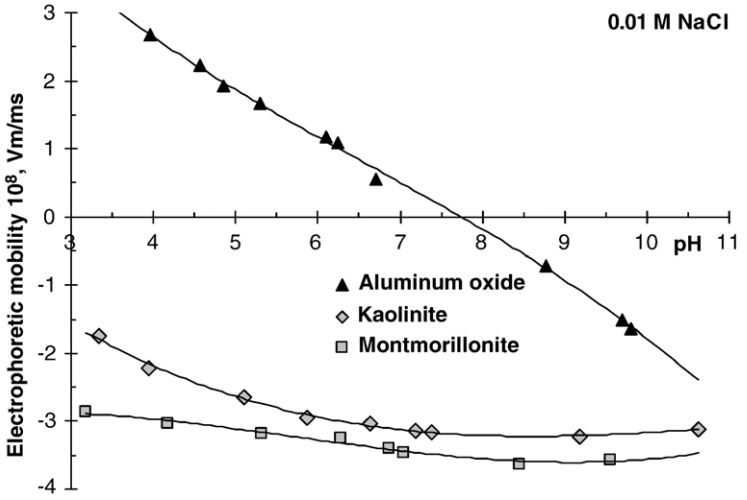

Fig. 8. pH-dependent charge state of clay particles in comparison with aluminum oxide; laser Doppler electrophoresis measured in dilute suspensions at 25 ± 0.1 °C.

followed by particle size determination. Dynamic light scattering (DLS) provides reliable size data even when the system is undergoing coagulation (Holthoff et al., 1996; James et al., 1992).

The pH-dependent hydrodynamic sizes calculated from the cumulant analysis of first order correlation functions are shown in Fig. 9. Comparing the measured data of kaolinite and montmorillonite, the characteristic difference in pH-induced particle aggregation in dilute suspensions containing only 0.01 M NaCl is obvious. The highly charged montmorillonite particles form stable suspension; apart from a slight increase below pH ~ 7, the average particle size is almost constant over the whole range of pH as explained elsewhere (Keren and Sparks, 1995; Tombácz et al., 1999, 2001). In principle the positively charged edges can interact with the negative basal plates below pH ~ 6.5, however, edge-to-face heterocoagulation does not take place at such a low ionic strength because the oppositely charged edge surfaces remain hidden due to the spillover of the dominant electric double layer on the face of montmorillonite plates (Tombácz and Szekeres, 2004). On the contrary, kaolinite particles, which have commensurable amounts of permanent and pH-dependent charges, strongly aggregate below the pH ~ 7, since the positively charged Al–OH sites especially at edges can interact with the negative basal plates forming edge-to-face aggregates (Van Olphen, 1963; Bartoli and Philippy, 1987; Zhao et al., 1991; Penner and Lagaly, 2001). In the destabilized suspensions, the measured particle size increased in time showing the progress of coagulation. Therefore, the measured larger sizes below the PZNPC of kaolinite in Fig. 9 are suitable only to compare a given kinetic state of coagulating systems.

3.3.2. Coagulation kinetics of kaolinite at different pHs

Coagulation kinetics measurements were performed to obtain exact data for the pH-dependent colloidal stability of fine kaolinite particles dispersed in indifferent electrolyte solution. Size evolution of aggregates in time was followed by dynamic light scattering. The initial slopes of hydrodynamic size vs. time curves were calculated at different electrolyte concentrations. The electrolyte concentration in each series was increased above the limit of fast coagulation (diffusion limited aggregation), where the initial slope of kinetic curves becomes independent of the electrolyte concentration. The stability ratio (w) was calculated from the initial slopes belonging to the slow and fast coagulation as suggested in literature (Holthoff et al., 1996; Kretzschmar et al., 1998).

The kinetic curves measured at pH ~ 4 were chosen as examples in Fig. 10 to show the existence of stable colloidal system, although it contains kaolinite particles with oppositely charged surface parts as explained above (Fig. 2). The size data measured at the lowest salt concentration (0.1 mmol l^{-1}) do not change in time, kaolinite particles can remain single for long time proving that no heterocoagulation takes place below a threshold of electrolyte concentration ~ 1 mmol l^{-1}. Above it, however, the extent of size increase in time becomes large even with a small increase in salt concentration, and the fast coagulation regime is reached at ~ 3 mmol l^{-1} NaCl. In a similar coagulation kinetics study of Kretzschmar et al. (1998), one (KGa-2) of the reference kaolinite of Clay Mineral Society was measured at pH ~ 4 and ~ 6. This kaolinite coagulated rapidly independent of electrolyte concentration from 1 to 100 mmol l^{-1} at both pH values

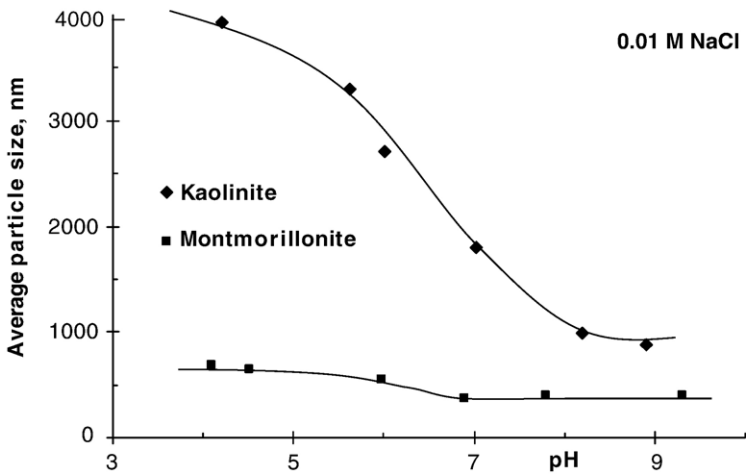

Fig. 9. Comparison of pH-dependent particle aggregation in kaolinite and montmorillonite suspensions; dynamic light scattering measured in dilute suspensions at 25 ± 0.1 °C. Clay samples: kaolinite from Zettlitz kaolin and Wyoming montmorillonite (Swy-2).

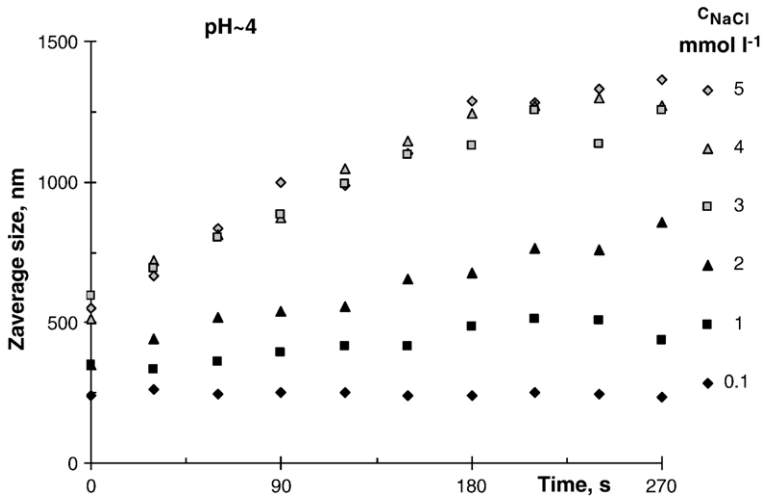

Fig. 10. Coagulation kinetics measured by dynamic light scattering: the size evolution of aggregates in kaolinite suspensions containing different NaCl concentrations at pH ~ 4, at 25 ± 0.1 °C. Sample: fine fraction of kaolinite.

contrarily to our finding in part, probably due to the significant difference between the kaolinite samples. The KGa-2 kaolinite is a poorly crystallized sample with low layer charges, its CEC is 3.3 meq/100 g (Van Olphen and Fripiat, 1979), while our sample from well-crystallized Zettlitz kaolin has about three times larger permanent charge (CEC ~ 9 meq/100 g).

The stability ratio values determined for the fine fraction of kaolinite at different pHs are plotted as a function of salt concentration in Fig. 11. The series of points show the typical curves with a slope of the slow coagulation regime and a plateau of the fast coagulation regime ($w \sim 1$). The critical coagulation concentration (c.c.c.) separates the fast from the slow coagulation regime. The estimated c.c.c. values are 3, 20 and 100 mmol l^{-1} NaCl at pH ~ 4, ~ 6 and above ~ 6.5, respectively. This colloidal stability results provide an indisputable proof for the pH-dependent stability of kaolinite, since the resistance of suspensions to electrolyte increases significantly with increasing pH of aqueous medium.

The enhanced stability is obvious especially at high pH ~ 8, where the amphoteric edge and O face sites of kaolinite particles have become negatively charged similarly to the sign of the permanent charges on T faces (Fig. 2). Although the probability of edge-to-face collisions is larger from hydrodynamic point of view, even in the

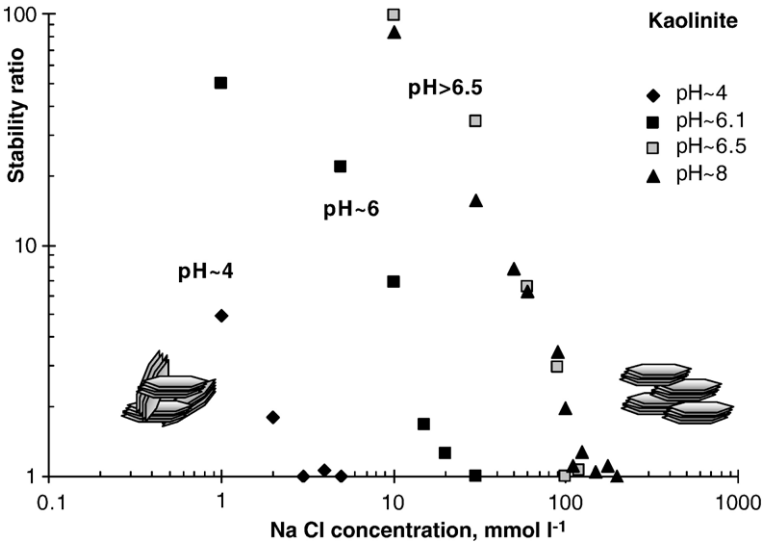

Fig. 11. pH-dependent sensitivity of fine fraction of kaolinite sols to indifferent electrolyte.

dispersion of the uniform negatively charged particles above the pH of PZNPC at pH ~ 6–6.5, the overlapping of the compressed edl on faces probably results in face-to-face oriented aggregates. The c.c.c. value ~ 100 mmol l^{-1} of kaolinite similar to that of montmorillonite (97–102 mmol l^{-1} at pH ~ 8.5) in our previous paper (Tombácz and Szekeres, 2004) shows that no significant difference in the colloidal stability of these clay minerals under slightly alkaline conditions. And so, we may conclude that the uniform edl charged negatively above the pH of $pH_{PZC,edge}$, used this unified term for both clays, does not differ from each other as depicted in Fig. 2 for kaolinite (bottom right) and montmorillonite (Tombácz and Szekeres, 2004). Since the charge density on particle surface has a determining role in the edl development, the robust kaolinite particles and the thin montmorillonite lamellae should have very similar surface charge density in the alkaline region. This seems to be supported by the enhanced deprotonation process resulting in negatively charged sites on kaolinite above pH ~ 7 as shown in Fig. 6 in comparison with montmorillonite. A c.c.c. value 85 ± 5 mmol l^{-1} measured at pH ~ 9.5 for the finest fraction of KGa-2 kaolinite was published recently in a delicate work (Berka and Rice, 2004), then the structure of aggregates formed in different regimes of coagulation was also identified (Berka and Rice, 2005). This c.c.c. smaller than ours involves less resistance against salt, so weaker colloidal stability of KGa-2 sample, which accords well with the above explanation, if we take into consideration that the permanent charge density of KGa-2 is about third that of Zettlitz kaolin.

The onset of edge-to-face coagulation at pH ~ 4 starts only above a threshold (~ 1 mmol l^{-1} NaCl) of electrolyte concentration, where the positively charged edge region of lamellae has emerged (Fig. 2) probably due to the change in the thickness of edl (Debye length ~ 10 nm in 1 mmol l^{-1} 1:1 electrolyte solution), since it becomes comparable with the thickness of kaolinite lamella (10–120 nm (Brady et al., 1996), 40–70 nm (Wan and Tokunaga, 2002)). Kaolinite forms stable suspension at very low ionic strengths, where Debye length is larger, and so the edls belonging to edges and faces may spill over. Under this condition (e.g. 0.1 mmol l^{-1} NaCl), the average particle sizes are constant (200–250 nm in Fig. 10) in time independently of the existence of oppositely charged parts on particles. In principle, the positively charged parts (edges and O faces) can interact with the negative T faces below pH ~ 6–6.5, however, edge-to-face heterocoagulation does not take place at very low ionic strength similarly to the case of oppositely charged magnetite and montmorillonite particles published previously (Tombácz et al., 2001). These coagulation kinetics studies showed that diffusion limited aggregation is induced by 1:1 electrolyte (NaCl) concentration larger than ~ 3 mmol l^{-1} at pH ~ 4, which is much lower, than 25–26 mmol l^{-1} determined for Swy-1 and -2 montmorillonite samples showing the different mechanisms due to substantial difference between the 1:1 type kaolinite and 2:1 type montmorillonite particles. While the spillover of the dominant double layer on the faces of thin lamellae seemed to be an acceptable mechanism for montmorillonite (Tombácz and Szekeres, 2004), it is not applied for the robust kaolinite particles at all.

The pH region near to $pH_{PZC,\ edge}$ ~ 6–6.5, where edges and O faces are probably uncharged, is very interesting in colloidal stability point of view. The kaolinite suspensions are highly sensitive to even a small change in pH in this region. Based on the pH-dependent partitioning study (Wan and Tokunaga, 2002), exactly the same was stated for KGa-1 sample, since kaolinite particles were able to accumulate at air–water interface only at pH ~ 6.3, which was enhanced below (pH ~ 5.7), but did not occur at all above (pH ~ 7.5) this pH. Our coagulation kinetics results at pH ~ 6 are shown in Fig. 11. The estimated c.c.c. value was about 20 mmol l^{-1} NaCl. However, a small increase in the pH of suspensions resulted in a sudden increase in the resistance against salt reaching the stability in alkaline region, e.g. the limit of fast coagulation was about at ~ 100 mmol l^{-1} NaCl, if the pH was increased by some tenths, to pH ~ 6.5. The probability of edge-to-face random collisions is larger than that of the face-to-face collisions in this pH region, too. However, the existence of different structure of aggregates, i.e. either edge-to-face or face-to-face arrangement of lamellae, in equilibrium state may be questionable. It seems no any driving force exists under these solution conditions to rearrange the in situ formed edge-to-face aggregates.

3.4. pH-dependent particle network formation in aqueous kaolinite suspensions

The formation of semi-solid materials and the mechanical properties of particle network in suspensions can be investigated by means of rheology. Here, the formation of pH-dependent structure in kaolinite suspensions at 0.01 M NaCl was studied. First, the steady-state flow curves determination, the most frequently used rheological measurement of aqueous clay suspensions, was used. The results obtained for 15 g/100 g suspensions of kaolinite at different pHs are shown in Fig. 12 and Table 2. The significant change in flow character with decreasing pH is obvious. It can be seen that curves run higher and higher, and the up- and downward curves are not identical, especially below pH ~ 7. The edges and O faces of kaolinite particles are negatively charged in alkaline suspension,

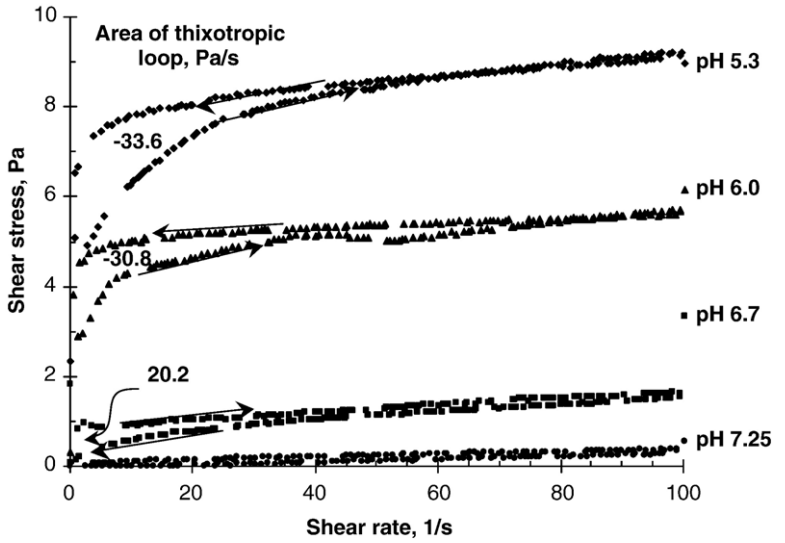

Fig. 12. Flow curves measured with an increasing (upward) then decreasing (downward) shear rate ramp for 15 g/100 g Na-kaolinite suspensions containing 0.01 M NaCl at different pHs above (●:7.25, ■: 6.7), at (▲: 6.0) and below (◆: 5.3) the pH of PZNPC (~6–6.5) of edges and O faces at 25± 0.1 °C.

therefore the whole surface holds similar charges. The uniformly charged particles repel each other, network cannot form, and so the stable kaolinite suspension shows shear thinning flow character with a very small thixotropy (bottom curve at pH ~ 7.25). A slight decrease in pH, but still above the PZNPC of kaolinite makes thixotropy definite, and the pseudoplastic flow character with small yield value also appears (curve at pH ~ 6.7). Further decrease in pH, reaching the uncharged then positively charged state of amphoteric sites at edges and O faces, however, causes a sudden change in suspension flow (curve at pH ~ 6.0). The above discussed results of coagulation kinetics also showed that kaolinite suspensions were highly sensitive even to a small change in pH in this region. Namely, the well-stabilized state was preserved down to pH ~ 6.5, but below it the stability of suspensions decreased drastically at pH ~ 6.1 due to the probability of edge-to-face interaction. In dense suspensions at pH ~ 6, semi-solid system forms, plastic flow becomes obvious, the increase in yield value is more than tenfold (Table 2), and an unexpected antithixotropic character (apparent viscosity belonging to downward curve is larger than that of upward curve) appears. This feature remains characteristic of suspension (uppermost curve at pH ~ 5.3) in acidic region showing the formation of strong attractive gels (Abend and Lagaly, 2000), here that of edge-to-face and face-to-face heterocoagulated network due to the attraction of oppositely charged parts (both edges and T faces, and O faces and T faces) of kaolinite particles. The area of antithixotropic loops increases slightly with decreasing pH. It is interesting to compare the time dependent, thixotropic/antithixotropic behavior of aqueous kaolinite and montmorillonite suspensions. In both cases the surface of clay particles has patch-wise charge heterogeneity under acidic conditions. Thixotropic gels formed in montmorillonite suspensions at pHs below the $pH_{PZC,edge}$ due to the formation of edge-to-face heterocoagulated network of very thin lamellae, which has definite elastic response, if only the applied stress is below the yield values as explained before (Tombácz et al., 2004; Tombácz and Szekeres, 2004). The edge-to-face network forms over a prolonged period, its structure breaks down gradually during shear ramp and cannot rebuild over the measuring time. Therefore smaller apparent viscosities belongs to the downward curve than that to the upward curve, i.e. hysteresis between up and down curves indicates and may measure thixotropy (positive values

Table 2
Evaluation of downward flow curves of 15 g/100 g kaolinite suspensions containing 0.01 M NaCl according to the Bingham model (Barnes et al., 1989)

Suspension pH	Flow character	Yield value Pa	Plastic viscosity Pa s	Thixotropic loop area Pa/s
7.25	Shear thinning	0	0.0030*	–
6.70	Pseudoplastic	0.66	0.0089	20.2
6.00	Plastic	5.10	0.0052	−30.8
5.30	Plastic	7.97	0.0116	−33.6

Note : * limited viscosity at higher shear rate.

assigned to the hysteresis area). On the contrary, the apparent viscosity increases slightly during shear ramp in the antithixotropic (negative values for loop area) kaolinite suspensions at and below pH ~ 6, where both the edges and the O faces hold certainly positive charges. Antithixotropy does not occur in montmorillonite suspensions, in which only the edges are negatively charged below pH ~ 6.5. To interpret the antithixotropic behavior of kaolinite suspensions, besides the formation of edge-to-face aggregates, we suppose a weaker attraction between the oppositely charged O and T faces of particles, because the positive charge formation due to the protonation of Al–OH sites on O faces is probably retarded as related to that on edges (Avena et al., 2003). Both types of heterocoagulated aggregates form in a random collision during suspension preparation, and no driving force is present to rearrange this particle network for even a long standstill. However, the weaker points of network, probably the adhered O and T faces, break first in the shear field, when shear rate is increased (upward curve), and edge-to-face aggregates can in situ form providing a slight increase in the shear tolerance of kaolinite suspension in the downward shear ramp.

The yield values calculated for kaolinite suspensions rise significantly with decreasing pH (Table 2), similarly to that measured in montmorillonite suspensions. The yield value is proportional to the mechanical strength of physical network and depends on the number and the strength of bondages between particles in unit volume of suspensions (Barnes et al., 1989). The lower the pH the larger the amount of positive charges on the edges and O faces of kaolinite plates, therefore the attraction between the positively charged edges and negative basal plates becomes stronger with decreasing pH.

We attempted to study on the viscoelastic properties of kaolinite suspensions in parallel to the montmorillonite as published previously (Tombácz et al., 2004). While both creep tests and forced oscillation measurements were successful in the case of montmorillonite proving the elastic behavior of thixotropic montmorillonite gels below the pH of edge PZC, the measurements do not show a clear viscoelastic feature for kaolinite suspensions below pH ~ 6. The elastic response of particle network was measurable only under static conditions. Some series of creep and recovery curves measured at different pHs and stresses are shown in Fig. 13. The pH-dependent behavior of kaolinite (Fig. 13 a) shows that alkaline suspension is essentially different from that of acidic ones in good harmony with the feature of flow curves (Fig. 12). An almost ideal Newtonian (liquid-like) behavior was detected for suspension containing uniformly charged particles at pH ~ 7.25, since deformation continually increased in a linear manner as long as the stress was applied, and there was no any restoration at all in the absence of attraction between particles. However, suspensions at pH ~ 6 and 5.3, where particle network can build in dense suspensions due to attractive forces between the oppositely charged parts of kaolinite plates, an elastic response in the jelly-like suspensions definitely appears. The contribution of elastic component to the viscoelastic deformation of sample is obvious, since the applied stress results in an instantaneous strain jump, which restores after releasing, but a significant non-recoverable deformation remains due to the presence of viscous component. Creep tests were used to analyze the recovery of structure in montmorillonite suspensions over the range of pH from ~ 3 to 9 (Durán et al., 2000), and as a function of ionic strength (Abend and Lagaly, 2000). Similar work was not found for kaolinite. Our creep tests proved that attractive particle network forms in acidic suspensions due to the electrostatic attraction between the oppositely charged parts of kaolinite plates, which has elasticity besides viscous properties. However, the shear stress tolerance of viscoelastic particle network is limited, and it has close relation with the yield values as shown for two suspensions having significantly different, low and high yield values in the b and c parts of Fig. 13. On the one hand, even a very weak particle network formed in dense kaolinite suspension at pH ~ 6.7 can exhibit some elasticity (more than 50% recovery showed on curve in Fig. 13 b), if it is deformed by smaller stress (0.1 Pa) than its yield value (0.66 Pa in Table 2), however, a liquid-like flow occurs at stronger effect (e.g. 1 Pa in Fig. 13 b). On the other hand, a strong particle network with dominant elastic response (about 90% recovery exhibited on curve belonging to pH ~ 5.3 and 1 Pa in Fig. 13 c) can liquefy, if the applied stress is larger than its tolerance, i.e. yield value ~ 8 Pa (creep curve measured at 10 Pa in Fig. 13 c). In accordance with the facts for thixotropic montmorillonite gels (Tombácz et al., 2004; Tombácz and Szekeres, 2004), it can be stated that an elastic response of particle network is expected in kaolinite suspensions, if only the applied stress is below the yield values. This last assumption was not emphasized in the previous papers (Durán et al., 2000; Abend and Lagaly, 2000), but creep tests were done at low constant stresses in both works (0.2 and 0.4 Pa, respectively).

The creep tests proved attractive gel formation in acidic suspensions, which has measurable elasticity besides viscous properties. However, the measurements under dynamic conditions failed, we could not find an appropriate region of linear viscoelasticity in the forced oscillation studies for the same suspensions. It seems that heterocoagulated network of robust kaolinite particles is

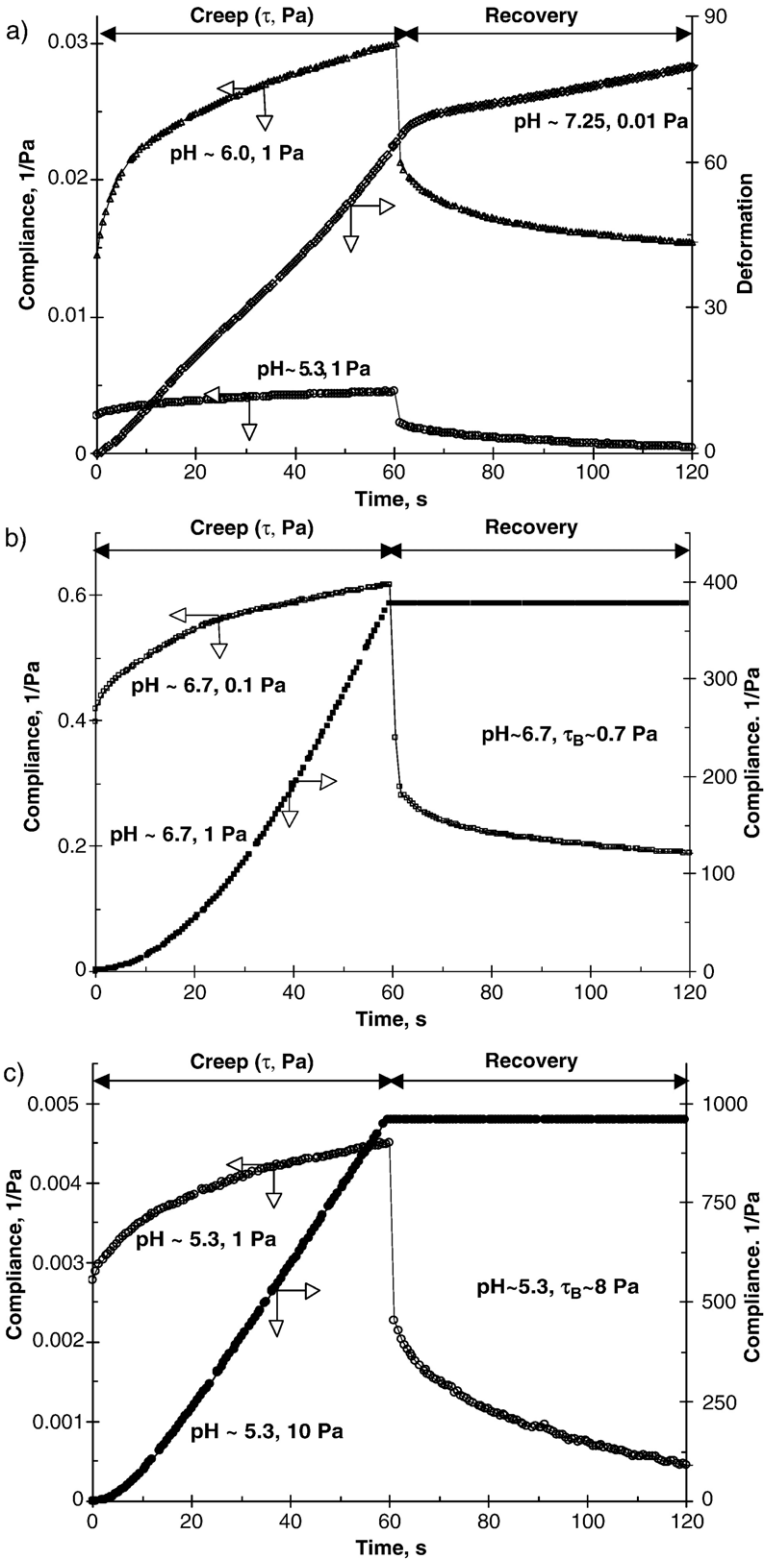

Fig. 13. Creep and recovery results for 15 g/100 g kaolinite suspensions containing 0.01 M NaCl at different pHs and stresses applied in creep test measurements at 25 ± 0.1 °C. Effect of suspension pH (a), and influence of applied stress below and above the yield value of weakly (b) and strongly (c) adhered particle networks.

fragile and rigid, and so it is substantially different from that of thin montmorillonite lamellae.

4. Conclusions

Clay mineral particles hold both permanent negative charges on faces and pH-dependent either negative or positive charges developing mainly on Al–OH active sites at the broken edges and exposed hydroxyl-terminated planes in general. Since these two types of sites are situated on the given parts of particle surface, different patches exist on the basal planes and edges of clay lamellae, and so the clay particles are the typical cases of patch-wise surface heterogeneity (Koopal, 1996; Tombácz, 2002). The size of patches and the lateral interactions of surface sites are important to develop patch-wise charge heterogeneity in aqueous medium, where hydration and ion adsorption smear out the electrostatic potential. With non-interacting patches each patch develops its own (smeared out) electrostatic potential (Koopal, 1996). We have stated that the surface charge heterogeneity is not a general feature of montmorillonite particles (Tombácz and Szekeres, 2004), now we attempt to summarize the facts for clay minerals in general, on the basis of the study on 2:1 type montmorillonite and 1:1 type kaolinite, which have essential differences originating from the crystal structure (TOT and TO) in the geometry and the layer charge density.

The patch-wise surface heterogeneity is inherent property of clay mineral particles owing to their crystal structure, the basal planes and edges of clay lamellae hold different surface sites in patches. The different patches of particle surface become charged in aqueous suspensions due to the hydration of clay surface itself and rather that of exchangeable cations (Johnston and Tombácz, 2002), and the interfacial acid–base reactions (Tombácz, 2002). Thus surface charge heterogeneity of clay particles may exist in aqueous suspensions. Surface charges are neutralized by a diffuse cloud of ions from electrolyte solutions. Electric double layers (edl) form on each patches; one type with constant charge density on the faces bearing permanent charges, and the other type with constant potential at constant pH on the parts of surface, where pH-dependent charges develop, mainly at the edges. Therefore the local electrostatic field formed around particles with different asymmetry in respect of both the aspect ratio and the surface charging of edges and faces is definitely determined by the crystal structure of clay particles. The electric fields on the different patches have mutual influence on processes. The electric field on faces due to charge defects in crystal lattice affects not only on ion distribution on basal planes, but also on surface charge formation at edges as stated previously (Avena et al., 2003).

The effect of pH and indifferent electrolytes on the development of surface charge heterogeneity on clay particle is simultaneous, none of them can be interpreted alone. The pH of aqueous medium has two kinds of specific role, one is the high affinity of H^+ ions to neutralize the permanent negative charges on faces, and the other is providing chemical species (H^+ and OH^-) to the surface protolytic reactions on broken edges and exposed hydroxyl-terminated planes, in which the pH-dependent edl forms. The fact that ion exchange reaction with H^+-ions always takes place with changing pH, but its extent is significantly influenced by the electrolyte concentration, results in a characteristic shift in the pH-dependent net proton surface excess curves measured with increasing ionic strength. The effect of electrolytes is also doubled, since cations are always involved in the ionexchange process, while both ions of electrolytes obey electrostatic constraints, i.e. take part in formation of diffuse (outer) part of electric double layers on each patch. With increasing electrolyte concentration, on the one hand the ionexchange equilibrium shifts, and on the other hand surface charge neutralization becomes more effective enhancing the charge formation on pH-dependent sites, besides the narrowing of all electric double layers. We should note that effect of decreasing salt content is opposite, and for example the exhausted or even a long dialysis of clay suspensions against pure water results in a fairly undefined state mainly in cationexchange, but in diffuse part of edls, too. A definite initial state of monocationic clay in aqueous suspension can be reached in equilibrium dialysis against dilute electrolyte solution, for example 0.01 M NaCl in the case of Na-montmorillonite and Na-kaolinite.

The existence of oppositely charged surface parts on particles is the most interesting question of the surface charge heterogeneity of clays in both theoretical and practical points of view. In general, it exists only in aqueous medium under acidic conditions, where Al–OH sites are protonated as proved at pHs below the point of zero charge (PZC) of edge sites (~6.5) for montmorillonite (Tombácz and Szekeres, 2004), and as showed at pHs below PZNPC ~ 6–6.5 involved both edge and O face sites for kaolinite in the present paper. Although the oppositely charged patches on clay particles are present in acidic suspensions, the positive and negative patches may not see, and so do not necessarily attract each other. Heterocoagulation becomes perceptible only above a threshold of electrolyte concentration, when electric double layers belonging to different patches remain localized on the faces and edges. This heterocoagulation threshold is

definitely influenced by the geometry and layer charge density of clay particles. The extreme geometry of montmorillonite lamellae (Table 1) allows that dominant edl extending from the particle faces spills over at low salt concentration, when the thickness of edl (Debye length, e.g. ~3 nm at 10 mmol l^{-1}) is larger than that of the thin lamella (~1 nm) and it remains localized on basal plane only at and above 20–30 mmol l^{-1} NaCl (Fig. 2 in Tombácz and Szekeres, 2004). This threshold for the robust kaolinite particles is very low, only ~1 mmol l^{-1} NaCl, where the positively charged edge region of lamellae has emerged (Fig. 2), and the onset of heterocoagulation starts probably due to the change in the thickness of edl (Debye length ~10 nm in 1 mmol l^{-1}), where it becomes comparable with the thickness of kaolinite lamella (10–120 nm (Brady et al., 1996). This heterocoagulation, mainly interaction between faces with constant charge density and edges with constant potential (at constant pH) as depicted in Fig. 1 seems to be a fairly unusual case in colloid stability point of view (Gregory, 1975).

The crystal structure of clay minerals governs the surface charge heterogeneity of particles dispersed in aqueous medium. The existence of oppositely charged patches depends characteristically on the pH, but its appearance in suspension properties depends on the electrolyte concentration of solution, too. The behavior of aqueous clay suspensions in the presence of indifferent electrolytes, even the accumulation of clay particles at air–water interface, and the film formation, the dispersion or aggregation of particles, the unique time dependent flow properties, especially thixotropy and viscoelastic gel formation, all these excellent properties can be tuned optionally in the knowledge of specific surface charge properties of clay particles.

Acknowledgements

This work was supported by the grant GOCE-CT-2003-505450. The authors are grateful to FLORIN Rt. Szeged, Hungary for providing Rheometer HAAKE RS150 at our services. We thank Clifford Johnston very much for drawing the atom arrangement in a two-layer mineral inserted in Fig. 1, and for the remarkable discussion on clays before.

References

Abend, S., Lagaly, G., 2000. Sol-gel transition of sodium montmorillonite dispersions. Appl. Clay Sci. 16, 201–227.

Akbour, R.A., Douch, J., Hamdani, M., Schmitz, P., 2002. Transport of kaolinite colloids through quartz sand: influence of humic acid, Ca2+, and trace metals. J. Colloid Interface Sci. 253, 1–8.

Appel, C., Ma, L.Q., Dean Rhue, R., Kennelley, E., 2003. Point of zero charge determination in soils via traditional methods and detection of electroacoustic mobility. Geoderma 113, 77–93.

Avena, M.J., De Pauli, C.P., 1998. Proton adsorption and electrokinetics of an Argentinean montmorillonite. J. Colloid Interface Sci. 202, 195–204.

Avena, M.J., Mariscal, M.M., De Pauli, C.P., 2003. Proton binding at clay surfaces in water. Appl. Clay Sci. 24, 3–9.

Barnes, H.A., Hutton, J.F., Walters, K., 1989. An Introduction to Rheology. Elsevier, Amsterdam.

Bartoli, F., Philippy, R., 1987. The colloidal stability of variable-charge mineral suspensions. Clay Miner. 22, 93–107.

Berka, M., Rice, J.A., 2004. Absolute aggregation rate constants in aggregation of Kaolinite measured by simultaneous static and dynamic light scattering. Langmuir 20, 6152–6157.

Berka, M., Rice, J.A., 2005. Relation between aggregation kinetics and the structure of kaolinite aggregates. Langmuir 21, 1223–1229.

Blockhaus, F., Séquaris, J.-M., Narres, H.D., Schwuger, M.J., 1997. Adsorption–desorption of acrylic-maleic acid copolymer at clay minerals. J. Colloid Interface Sci. 186, 234–247.

Bolland, M.D.A., Posner, A.M., Quirk, J.P., 1980. pH-independent and pH-dependent surface charges on kaolinite. Clays Clay Miner. 28, 412–418.

Bolt, G.H., Bruggenwert, M.G.M. (Eds.), 1978. Soil Chemistry A. Basic Elements. Elsevier, Amsterdam.

Brady, P.V., Cygan, R.T., Nagy, K.L., 1996. Molecular controls on kaolinite surface charge. J. Colloid Interface Sci. 183, 356–364.

Brown, W. (Ed.), 1993. Dynamic Light Scattering. Oxford University Press, New York.

Coppin, F., Berger, G., Bauer, A., Castet, S., Loubet, M., 2002. Sorption of lanthanides on smectite and kaolinite. Chem. Geol. 182, 57–68.

Dangla, P., Fen-Chong, T., Gaulard, F., 2004. Modelling of pH-dependent electro-osmotic flows. C.R. Mecanique 332, 915–920.

Durán, J.D.G., Ramos-Tejada, M.M., Arroyo, F.J., Gonzáles-Caballero, F., 2000. Rheological and electrokinetic properties of sodium montmorillonite suspensions - I. Rheological properties and interparticle energy of interaction. J. Colloid Interface Sci. 229, 107–117.

Everett, D.H., 1986. Reporting data on adsorption from solution at the solid/solution interface. Pure Appl. Chem. 58, 967–984.

Gregory, J., 1975. Interaction of unequal double layers at constant charge. J. Colloid Interface Sci. 51, 44–51.

Herrington, T.M., Clarke, A.Q., Watts, J.C., 1992. The surface charge of kaolin. Colloids Surf. 68, 161–169.

Holthoff, H., Egelhaaf, S.U., Borkovec, M., Schurtenberger, P., Sticher, H., 1996. Coagulation rate measurements of colloidal particles by simultaneous static and dynamic light scattering. Langmuir 12, 5541–5548.

Hu, Y., Jiang, H., Wang, D., 2003. Electrokinetic behavior and flotation of kaolinite in CTAB solution. Miner. Eng. 16, 1221–1223.

Hunter, R.J., 1981. Zeta Potential in Colloid Science, Principles and Applications. Academic Press, London.

James, R.O., Parks, G.A., 1982. Characterization of aqueous colloids by their electrical double-layer and intrinsic surface chemical properties. In: Matijevic, E. (Ed.), Surface and Colloid Science, vol. 12. Plenum, New York, pp. 119–216.

James, M., Hunter, R.J., O'Brien, R.W., 1992. Effect of particle size distribution and aggregation on electroacoustic measurements of zeta-potential. Langmuir 8, 420–423.

Johnston, C.T., Tombácz, E., 2002. Surface chemistry of soil minerals. In: Dixon, J.B., Schulze, D.G. (Eds.), Soil Mineralogy with Environmental Applications. Soil Science Society of America, Madison, Wisconsin, USA, pp. 37–67.

Keren, R., Sparks, D.L., 1995. The role of edge surfaces in flocculation of 2:1 clay minerals. Soil Sci. Soc. Am. J. 59, 430–435.

Koopal, L.K., 1996. Ion Adsorption on Mineral Oxide Surfaces. In: Dabrowski, A., Tertykh, V.A. (Eds.), Adsorption on New and Modified Inorganic Sorbents in Studies in Surface Science and Catalysis, vol. 99. Elsevier, Amsterdam, pp. 757–796.

Kraepiel, A.M.L., Keller, K., Morel, F.M.M., 1998. On the acid–base chemistry of permanently charged minerals. Environ. Sci. Technol. 32, 2829–2838.

Kraepiel, A.M.L., Keller, K., Morel, F.M.M., 1999. A model for metal adsorption on montmorillonite. J. Colloid Interface Sci. 210, 43–54.

Kretzschmar, R., Holthoff, H., Sticher, H., 1998. Influence of pH and humic acid on coagulation kinetics of kaolinite: a dynamic light scattering study. J. Colloid Interface Sci. 202, 95–103.

Leroy, P., Revil, A., 2004. A triple-layer model of the surface electrochemical properties of clay minerals. J. Colloid Interface Sci. 270, 371–380.

Ma, C., Eggleton, R.A., 1999a. Cation exchange capacity of kaolinite. Clays Clay Miner. 47, 174–180.

Ma, C., Eggleton, R.A., 1999b. Surface layer types of kaolinite: a high-resolution transmission electron microscope study. Clays Clay Miner. 47, 181–191.

Mohan, K.K., Fogler, H.S., 1997. Effect of pH and layer charge on formation damage in porous media containing swelling clays. Langmuir 13, 2863–2872.

Penner, D., Lagaly, G., 2001. Influence of anions on the rheological properties of clay mineral dispersions. Appl. Clay Sci. 19, 131–142.

Schroth, B.K., Sposito, G., 1997. Surface charge properties of kaolinite. Clays Clay Miner. 45, 85–91.

Schulze, D.G., 2002. An introduction to soil mineralogy. In: Dixon, J.B., Schulze, D.G. (Eds.), Soil Mineralogy with Environmental Applications. Soil Science Society of America, Madison, Wisconsin, USA, pp. 1–35.

Sposito, G., 1984. The Surface Chemistry of Soils. Oxford University Press, New York.

Tombácz, E., 2002. Adsorption from Electrolyte Solutions. In: Tóth, J. (Ed.), Adsorption: Theory, Modeling, and Analysis. Marcel Dekker, New York, pp. 711–742.

Tombácz, E., 2003. Effect of environmental relevant organic complexants on the surface charge and the interaction of clay mineral and metal oxide particles. In: Bárány, S. (Ed.), Role of Interfaces in Environmental Protection. NATO ASI Series, Kluwer Academic Publisher, Dordrecht, pp. 397–424.

Tombácz, E., Szekeres, M., 2001. Interfacial acid–base reactions of aluminum oxide dispersed in aqueous electrolyte solutions. 1. Potentiometric study on the effect of impurity and dissolution of solid phase. Langmuir 17, 1411–1419.

Tombácz, E., Szekeres, M., 2004. Colloidal behavior of aqueous montmorillonite suspensions: the specific role of pH in the presence of indifferent electrolytes. Appl. Clay Sci. 27, 75–94.

Tombácz, E., Ábrahám, I., Gilde, M., Szántó, F., 1990. The pH-dependent colloidal stability of aqueous montmorillonite suspensions. Colloids Surf. 49, 71–80.

Tombácz, E., Szekeres, M., Kertész, I., Turi, L., 1995. pH-dependent aggregation state of highly dispersed alumina, titania and silica particles in aqueous medium. Prog. Colloid Polym. Sci. 98, 160–168.

Tombácz, E., Filipcsei, G., Szekeres, M., Gingl, Z., 1999. Particle aggregation in complex aquatic systems. Colloids Surf., A 151, 233–244.

Tombácz, E., Csanaky, Cs., Illés, E., 2001. Polydisperse fractal aggregate formation in clay and iron oxide suspensions, pH and ionic strength dependence. Colloid Polym. Sci. 279, 484–492.

Tombácz, E., Nyilas, T., Libor, Zs., Csanaki, Cs., 2004. Surface charge heterogeneity and aggregation of clay lamellae in aqueous suspensions. Prog. Colloid Polym. Sci. 125, 206–215.

Van Olphen, H., 1963. An Introduction to Clay Colloid Chemistry. Interscience, New York.

Van Olphen, H., Fripiat, J.J., 1979. Data handbook for clay materials and other non-metallic minerals. Pergamon Press, Oxford.

Wan, J., Tokunaga, T.K., 2002. Partitioning of clay colloids at air–water interface. J. Colloid Interface Sci. 247, 54–61.

Zhao, H., Low, P.F., Bradford, J.M., 1991. Effects of pH and electrolyte concentration on particle interaction in 3 homoionic sodium soil clay suspensions. Soil Sci. 151, 196–207.

Zhou, Z., Gunter, W.D., 1992. The nature of the surface charge of kaolinite. Clays Clay Miner. 40, 356–368.